Electronic Supplementary Information

A saponification triggered gelation of ester based Zn(II) complex through conformational transformations

Ashish Kumar, Mrigendra Dubey, Amit Kumar and Daya Shankar Pandey*

Department of Chemistry, Faculty of Science, Banaras Hindu University, Varanasi -221 005 (U.P.), India

Table of Contents: **Pages**

EXPERIMENTAL SECTION

Materials and Physical Methods

The solvents were thoroughly dried and distilled by standard literature methods prior to their use.[1] All the chemicals were purchased from Sigma Aldrich Chemical Co. Pvt. Ltd. and used as received. The ligand diethyl−5−(2−hydroxybenzylidene)−aminoisophthalate (**HL**) needed for the synthesis of **1** was synthesized and characterized following our earlier method.[2] The characterization details of **HL** and **1** are described below.

Elemental analyses for C, H and N were obtained on an Exeter Analytical Inc. CE−440 analyser. Infrared and electronic absorption spectra were acquired on a Perkin−Elmer−577 FT−IR and Shimadzu UV−1601 spectrophotometers, respectively. Fluorescence spectra at room temperature (rt) were recorded on a PerkinElmer Fluorescence Spectrometer (LS-55) and an integrated peltier system was used for variable temperature experiments. The life-time measurements were made using a TCSPC system from Horiba Yovin (Model: Fluorocube-01-NL). The samples were excited at 343 nm using a pico-second diode laser (Model: Pico Brite-375L). The data analysis was performed using IBH DAS (version 6, HORIBA Scientific, Edison, NJ) decay analysis software. ^{1}H (300 MHz) and ^{13}C NMR spectra (75.45 MHz) were obtained on a JEOL AL 300 FT−NMR spectrometer at rt using tetramethylsilane [$Si(CH_3)_4$] as an internal reference. Variable temperature (VT) NMR experiment was performed on Bruker Avance 400 MHz Switzerland using HR-MAS probe. High resolution mass spectra (HRMS) were acquired on a WATERS−Q−Tof Premier spectrometer. AFM images were captured on a NTMDT Solver NEXT Russia. SEM and TEM images were captured on JSM−7600F Field Emission Gun−Scanning Electron Microscope (FEG−SEM) and 120 kV ultra modern Transmission Electron Microscope of FEI. Powder X-ray diffraction data was collected on a Rigaku Smart Lab diffractometer between angle 4−60°.

UV/vis Study: Stock solution of **1** (50 μM) for electronic absorption study was prepared in $CHCl_3$. Solution of NaOH (2M) was prepared in methanol. We have taken optimum concentration of **1** as much close as gelation concentration (0.02 M) within instrument limits to observe certain effects on addition of NaOH. In a typical titration, solution of **1** was taken in a quartz cuvette (3.0 mL; path length, 1 cm) and NaOH solution added gradually with the help of a micropipette. After each addition, proper mixing was performed and spectra

recorded after 2 min and repeated thrice. VT absorption spectra of diluted gel (**IGM**; *c*, ~4.0 x 10^{-4} M) in temperature range from 25 - 70 ºC has been performed on a peltier system.

Fluorescence Study: Stock solution of **1** (20 mM) in $CHCl_3$ and 2M solution of NaOH was prepared in methanol for fluorescence study. All the experiments were performed on concentrations at which tight gelation occurs (*c*, 2.0 x 10^{-2} M) with adjusted slit widths to keep intensity within the instrument range. The limit of quantification observed was 1.0:0.2 to ~1.0:4.0 for **1**: NaOH. Characteristic fluorescence band of **1** at 1.5 x 10^{-5} M concentration appeared at 496 nm (λ_{ex}, 343 nm) and at with a large Stokes shift of ~156 nm which has been justified by fluorescence life-time measurements (~2.8 ns).

Theoretical Studies: Quantum chemical calculations have been performed using a hybrid version of DFT methods, namely B3LYP.[3] Basis set 6-31G** has been used for C, H, N and O, while LANL2DZ for Zn which combines quasi-relativistic effective core potentials with a valence double basis-set.[4] The geometry optimization and frequency calculations (to verify a genuine minimum energy structure) for **1** and its carboxylate analogue sodium salt **2** and Cu^{2+} analogue of complex **2** were performed using Gaussian 09 programme.[5]

Rheological Study: Measurements were carried out on a stress-controlled rheometer (Anton Paar Quality Control Rheometer Rheolab QC instrument) equipped with stainless steel parallel plates (20 mm dia., 0.2 mm gap) using freshly prepared gels (1.4 % w/v). Linear visco-elastic regions for the sample was determined by measuring storage modulus, G′ (associated with energy storage), and loss modulus G″ (associated with the loss of energy) as a function of the stress amplitude. Dynamic oscillatory work was kept at a frequency of 1 rad s^{-1}. Following tests were performed: increasing amplitude of oscillation up to 100% apparent strain on shear, time and frequency sweeps at 20 °C (20 min and from 0.1 to 10 rad s^{-1}, respectively), and a heating run to 100 °C at a scan rate of 1°C min^{-1}. All the measurements were conducted in triplicate.

Synthesis and characterization

Synthesis of complex [Zn(L_2)] (1): $Zn(NO_3)_2{\cdot}6H_2O$ (1.492 g, 5.0 mmol) dissolved in methanol (10 mL) was added to a methanolic solution of deprotonated $\mathbf{L^-}$ [obtained by treatment of **HL** (3.410 g, 10.0 mmol) with KOH (0.560 g, 10.0 mmol) and stirring in MeOH, (50 mL)] and resulting solution stirred at rt for an additional 3 h. Slowly, a yellow

precipitate separated which was filtered, washed with methanol, diethyl ether and dried under vacuum. Yield (2.496 g; 67%). Anal. Calcd. for [$C_{38}H_{36}N_2O_{10}Zn$]: C, 61.17; H, 4.86; N, 3.75; Found C, 61.13; H, 4.82; N, 3.77. IR (KBr pellets, cm^{-1}): 2980 (m, $\nu_{str}C–H_{aliphatic}$), 1717 (vs, $\nu_{str}C=O_{ester}$), 1610(s, $\nu_{str}C=N$). ^1H NMR ($CDCl_3$, 300 MHz, δ_H, ppm): 8.49 (s, 2H, *H*4), 8.46 (s, 2H, *H*1), 8.00 (s, 4H, *H*2 and *H*3), 7.42 (t, 2H, *J* = 7.9 Hz, *H*7), 7.24 (d, 2H, *J* = 7.2 Hz, *H*5), 6.96 (d, 2H, *J* = 8.4 Hz *H*8), 6.69 (t, 2H, *J* = 7.3 Hz, *H*6), 4.28 (q, 8H, *J* = 6.9 Hz, *H*9 and *H*11), 1.28 (t, 12H, *J* = 6.9 Hz, *H*10 and *H*12). ^{13}C NMR ($CDCl_3$, 75.45 MHz, δ_C, ppm): 165.2, 164.0, 163.7, 152.4, 148.4, 145.7, 132.3, 130.7, 129.1, 128.9, 128.2, 128.1, 126.2, 122.6, 118.6, 118.2, 61.8, 61.7, 61.5, 14.3. HRMS (TOF MS). Calcd, found: *m/z* 745.1740, 745.1730 [$(M+H)^+$]. UV/vis. (*c*, 50 μM; $CHCl_3$, λ_{max} nm, ε M^{-1} cm^{-1}): 343 (2.59×10^4) and 275 (3.61×10^4).

Synthesis of the gel (IGM): Stock solution of **1** (*c*, 20 mM in $CHCl_3$) and NaOH (*c*, 2.0 M in MeOH) were prepared and filtered to obtain a clear solution. For gelation a solution of NaOH (4.0 equiv) was added to a freshly prepared solution of **1** (1.0 mL) with 1 or 2 strokes of shaking. Almost instantaneously (within a minute) it gave a translucent, thermoreversible inorganic gel material (**IGM**).

Syntheses of analogous complexes: These were synthesized following the above procedure for **1** using respective metal nitrates [$Cd(NO_3)_2·6H_2O$ (0.357 g, 1 mmol) for [$Cd(L_2)$], Yield (0.380 g; 48%); $Cu(NO_3)_2·2.5H_2O$ (0.232 g, 1 mmol) for [$Cu(L_2)$], Yield (0.409 g; 55%); $Co(NO_3)_2·6H_2O$ (0.291 g, 1 mmol) for [$Co(L_2)$] Yield (0.310 g; 42%); and $Ni(NO_3)_2·6H_2O$ (0.291 g, 1 mmol) for [$Ni(L_2)$] Yield (0.362 g; 49%)]. The complexes were isolated as precipitates (powder) of light yellow, green, orange and yellow green, respectively. Anal. Calcd. for [$C_{38}H_{36}N_2O_{10}Cd$]: C, 67.55; H, 4.58; N, 3.53; Found C, 67.51; H, 4.62; N, 3.50. IR (KBr pellets, cm^{-1}): 2927–2976 (m, $\nu_{str}C–H_{aliphatic}$), 1728 (vs, $\nu_{str}C=O_{ester}$), 1609 (s, $\nu_{str}C=N$). Anal. Calcd. for [$C_{38}H_{36}N_2O_{10}Cu$]: C, 61.32; H, 4.88; N, 3.76; Found C, 61.29; H, 4.89; N, 3.77. IR (KBr pellets, cm^{-1}): 2980 (m, $\nu_{str}C–H_{aliphatic}$), 1717 (vs, $\nu_{str}C=O_{ester}$), 1610 (s, $\nu_{str}C=N$). Anal. Calcd. for [$C_{38}H_{36}N_2O_{10}Co$]: C, 61.71; H, 4.91; N, 3.79; Found C, 61.68; H, 4.88; N, 3.81. IR (KBr pellets, cm^{-1}): 2930–2977 (m, $\nu_{str}C–H_{aliphatic}$), 1717 (vs, $\nu_{str}C=O_{ester}$), 1610 (s, $\nu_{str}C=N$). Anal. Calcd. for [$C_{38}H_{36}N_2O_{10}Ni$]: C, 61.73; H, 4.91; N, 3.79; Found C, 61.71; H, 4.90; N, 3.75. IR (KBr pellets, cm^{-1}): 2928–2981 (m, $\nu_{str}C–H_{aliphatic}$), 1724 (vs, $\nu_{str}C=O_{ester}$), 1609 (s, $\nu_{str}C=N$).

Discussion

To pin point the changes occurring during sol-gel conversion on experimental ground as much as close to reality the fluorescence experiment was performed at high concentrations. As a strict precaution, experimental parameters were kept identical every time, so that any deviation due to high concentration, if any, would become invariable and spectral changes pertain only to the sol-gel conversion. To authenticate the said strategy, we have compared fluorescence spectra of **1** at different concentrations (2.0 x 10^{-2} M to 3.9 x 10^{-5} M). It shows a regular decrease in fluorescence intensity with a simultaneous blue shift with dilution (Fig. S7d). At ~3.9 x 10^{-5} M, a blue shift of ~14 nm noticed (λ_{em}, 496 nm), which indicated that emission maximum of the monomeric species for **1** should be < 510 nm but, conversely, it also supports that at 0.02 M concentration the monomer species do not raze its identity completely, rather attains some inter-planar weak interactions that is yet insufficient to form a viscous gel material. Similar effect of dilution has also been observed with **IGM** from an analogous experiment in the concentration range ~2.0 x 10^{-2} - ~1.5 x 10^{-4} M (Fig. S7f).

Further, it prompted us to perform a fluorescence titration experiment between **1** and NaOH under diluted conditions (*c*, 5.0 x 10^{-5} M, same as that for UV/vis) to compare and contrast the results with the concentrated one. Under diluted condition (*c*, 5.0 x 10^{-5} M), emission maximum appeared at ~496 nm (*vide supra*) which further showed significant decrease in the intensity with a maximum red shift of ~13 nm on addition of NaOH (excess). Despite a disparity in the positions of emission band ($\lambda_{em}^{0.02\ M}$, 510 nm; $\lambda_{em}^{50\ \mu M}$, 496 nm) it has been noticed that complex **1** exhibits similar changes in fluorescence intensity and red shift ($\Delta\lambda^{0.02\ M}$, 16 nm; $\Delta\lambda^{50\ \mu M}$, 17 nm) upon treatment with NaOH (Fig. S7e). This clearly indicated that under diluted conditions too, **1** undergoes structural and conformational transformations and increase in π-stacking similar to the one observed at higher concentration (0.02M). However, excess NaOH needed to observe the particular changes at 50 μM, signify that dilution greatly affects quick and stoichiometric response toward these changes and above all, never achieves a viscous gel state. Therefore, above experiments justify reliability of the fluorescence studies carried out at 0.02 M concentration.

The fluorescence decay is described as a sum of exponential functions. Average life time of bi-exponential fluorescence decay can be explained as -

$$\tau_{av} = a_1\tau_1 + a_2\tau_2$$

where, τ_{av} is average lifetime, a_1 and a_2 correspond to relative normalised amplitude of τ_1 and τ_2, τ_1 and τ_2 are two different lifetime components. a_1+a_2=1 always.

The average fluorescence lifetime for **1** at ~5 x 10^{-5} M has been measured as τ_{av} = 2.831 ns which has two lifetime components τ_1 and τ_2. The best fit values of lifetime components for τ_{av} = 2.831 ns can be explicated as –

$$2.831 = 0.70*2.43 + 30*3.75$$

The quality of fitted parameters were judged by reduced chi square (χ^2) values and corresponding residual distribution. To obtain the best fitting, χ^2 was kept near to unity.[6]

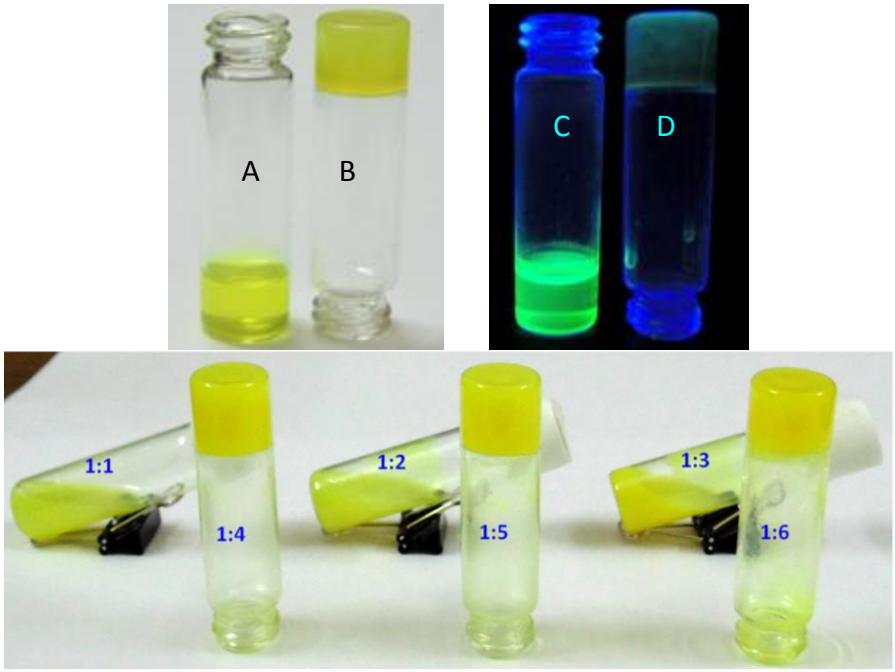

(E)

Figure S1. Photographs of (A) **1**, (B) **IGM** in inverted *vial* under naked eye and (C) **1**, (D) **IGM** in inverted vial under UV light (λ= 365 nm).; (E) Optimization of stoichiometric ratio of **1**: NaOH for creating a strong gel (pictures taken after 15 minutes).

Figure S2. Left to right in the order, (Zn(II), Cd(II), Cu(II), Co(II) and Ni(II), top). Formation of gelatinous precipitates with Cu(II), Co(II) and Ni(II) nitrate from left to right slanting vials, bottom. Pictures were taken after 15 minutes from addition of NaOH.

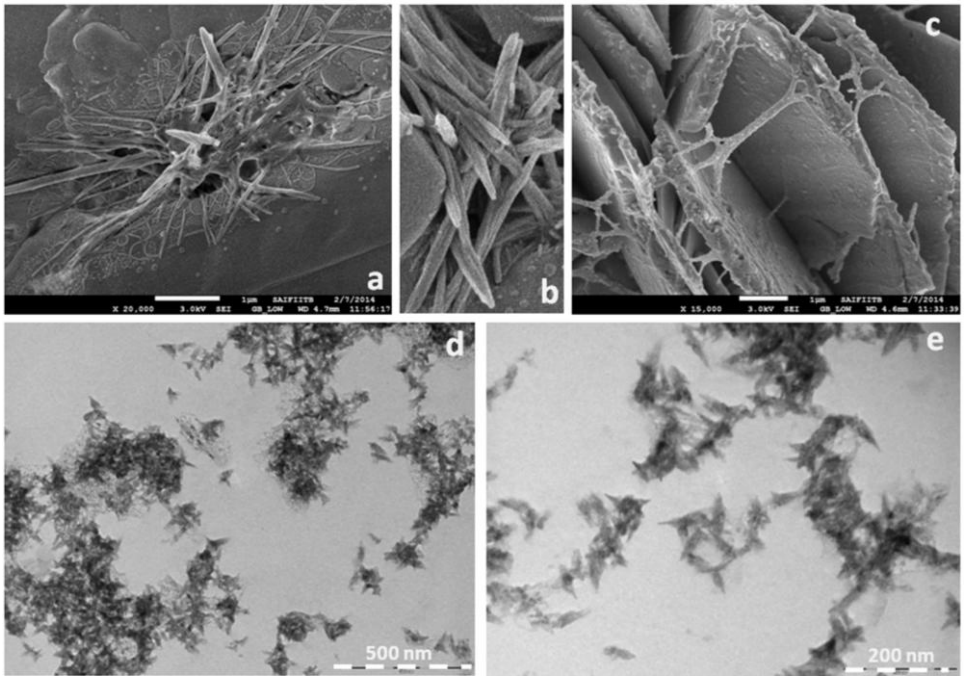

Figure S3. (a, b and c) Scanning electron micrographs (SEM) of **IGM** xerogels. 'a' denotes a group of fibers, 'b' a magnified (25,000x) cropped part of 'a' ; and 'c' shows the cross section image of xerogel at 15,000x. magnification (d and e). Transmission electron micrographs of diluted gel (~$1x10^{-4}$ M) clearly showing nano aggregates like architectures and all in a definite shape and aligned unidirectionally.

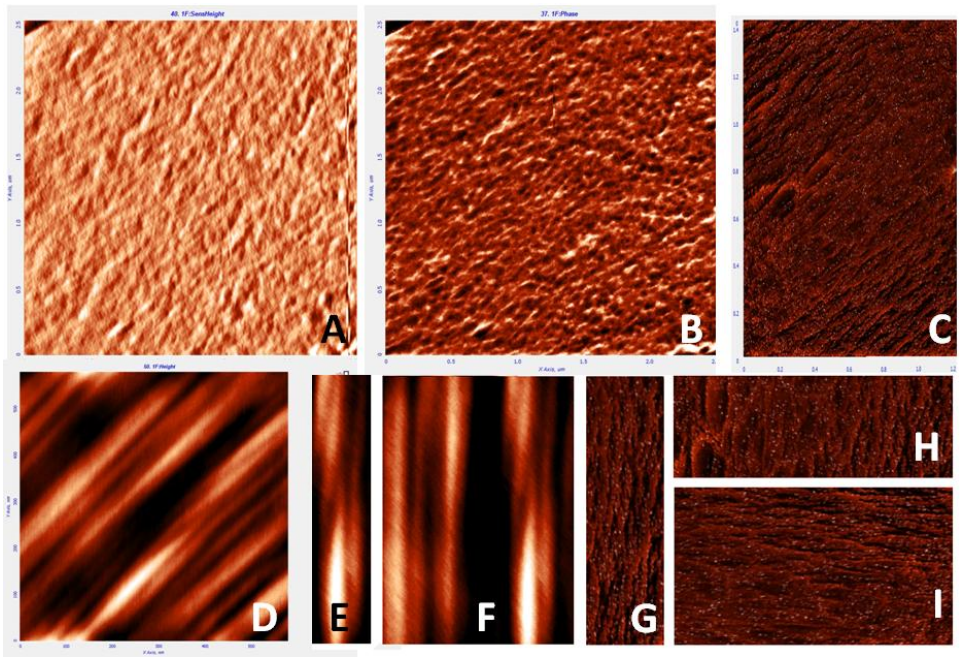

Figure S4. AFM image of the gel (**IGM**); Fibrous morphology observable for diluted gel ($1x10^{-3}$ M), (A) height image; (B) phase image; (C) 2D light image (cropped); (D) magnified image from A reveals many single fibers aligned in parallel manner; (E,F) cropped images showing single fibers and; (G,H,I) cropped images from 2D light view. Samples were prepared by spin-casting on mica before taking the AFM images.

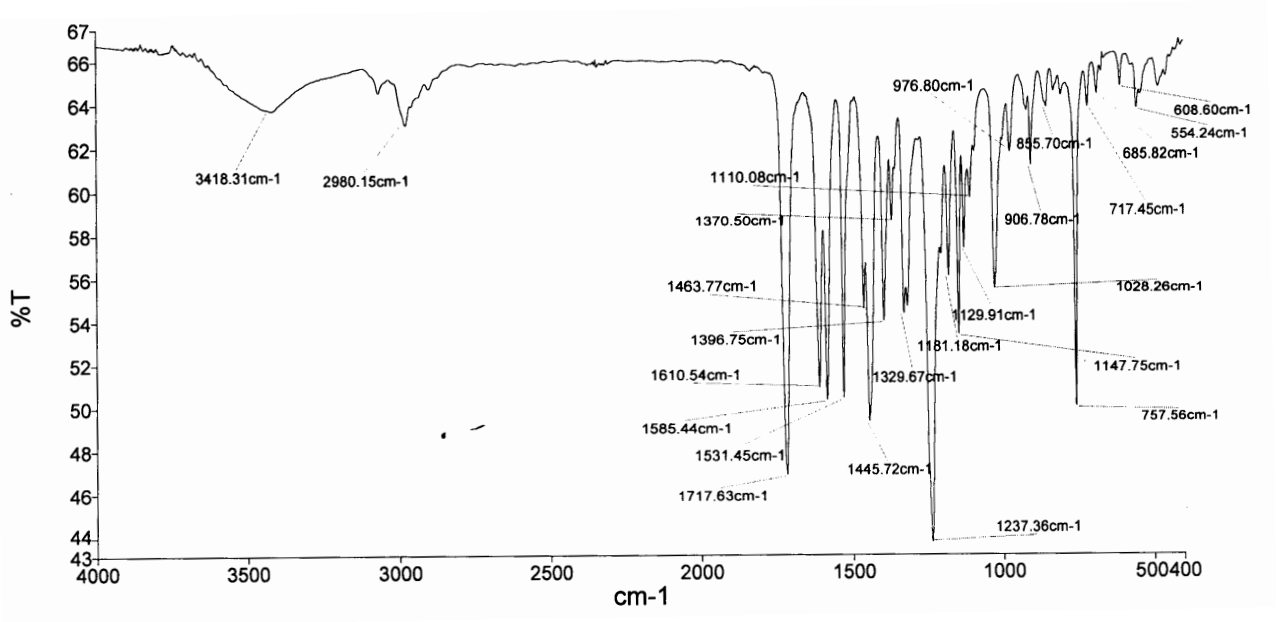

(a)

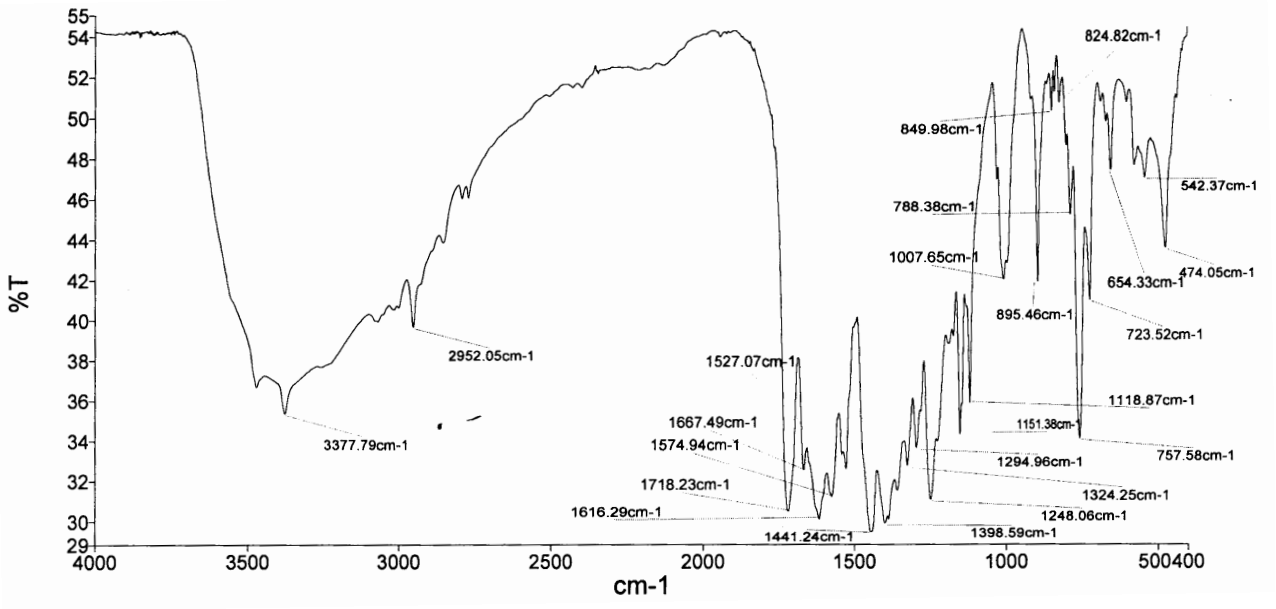

(b)

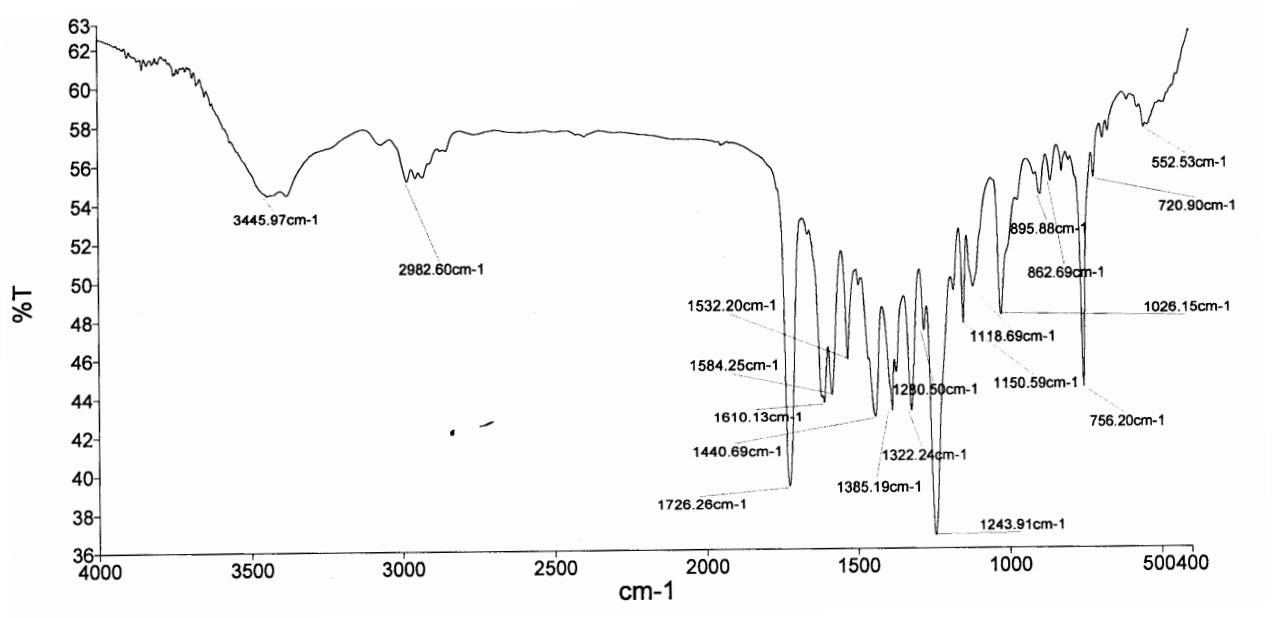

(c)

Figure S5. (a) Infrared spectrum of **1**, (b) **1**+ NaOH (**IGM**) and (c) **1**+ LiOH (Sol).

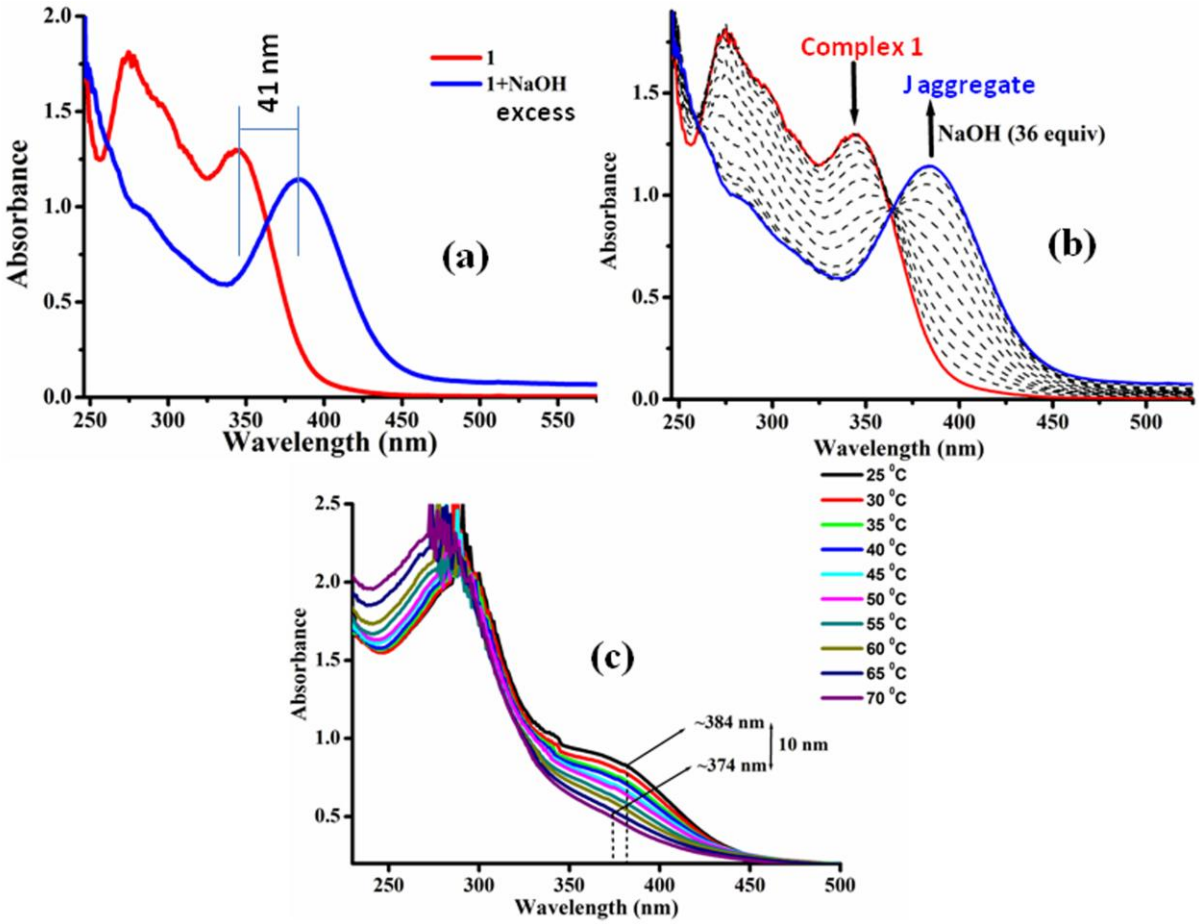

Figure S6. (a) UV/vis spectrum of **1** in $CHCl_3$ (*c*, 5.0 × 10^{-5} M) and **1**+NaOH (excess) at room temperature showing significant red shift of 41 nm indicating conformational change; (b) Titration spectra of **1** *vs* NaOH exhibiting gradual appearance of a new band at 384 nm attributable to J–aggregates and saturation at ~36 equiv; (c) Variable temperature UV/vis spectra of diluted gel (**IGM**; *c*, ~4.0 x 10^{-4} M) between 25 ºC to 70 ºC. Gel (**IGM**) has been diluted to such concentration that the band associated with aggregation (λ, ~384 nm) should appear as well as lie under the accepted range of optical density. With increasing temperature absorption band exhibited a substantial hypsochromic shift ($\Delta\lambda$, 10 nm) associated with reduction in optical density. It may be ascribed to the infringement of gel matrix at high temperature. The hypsochromic shift while breaking of aggregation confirms the involvement of J-aggregates.

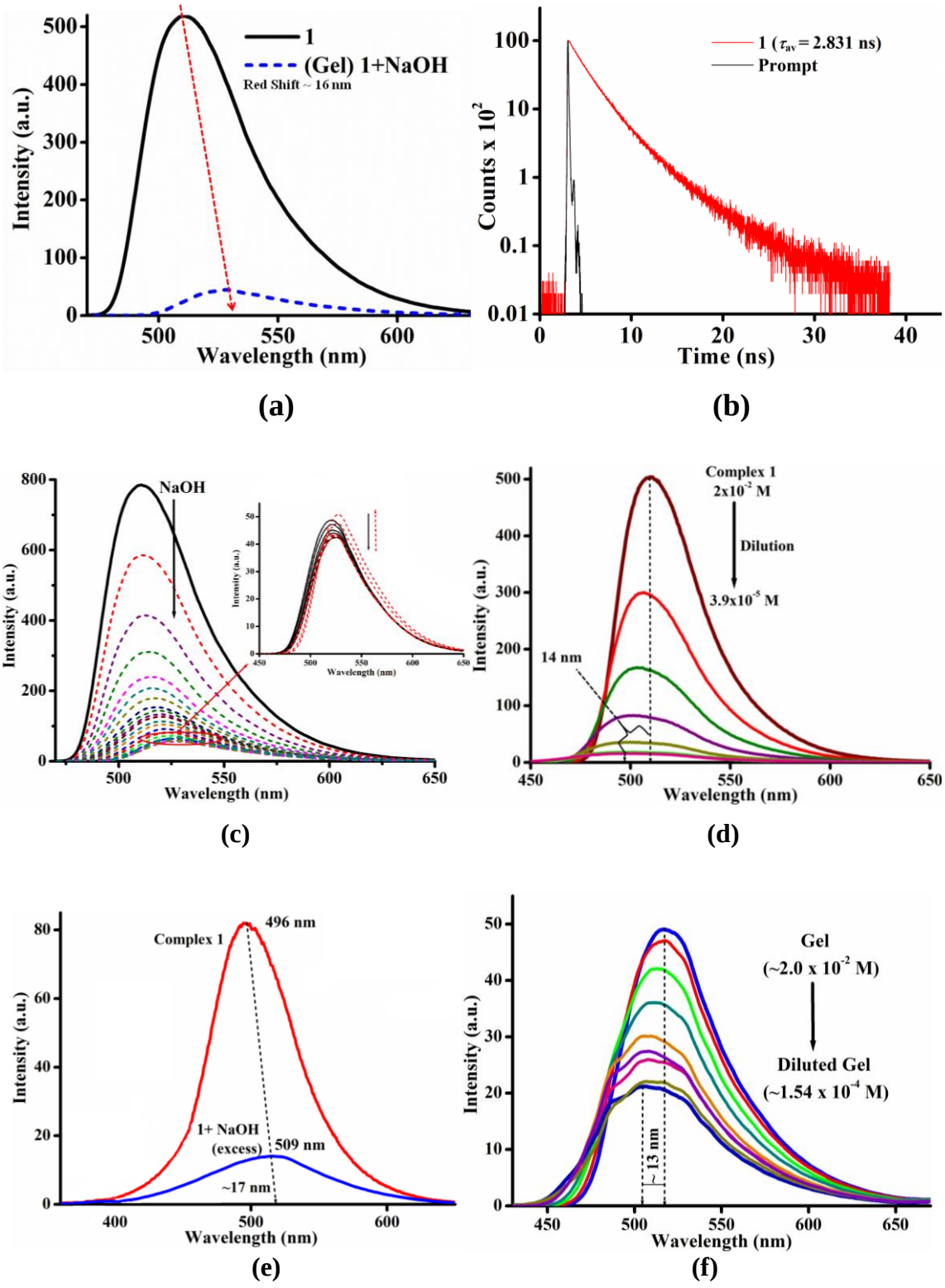

Figure S7. (a) Fluorescence spectra of **1** (black) and **1**+NaOH (dotted blue) displayed final red shift of 16 nm; (b) Fluorescence life time curve for **1** (τ_{av} ~2.8 ns); (c) Fluorescence titration of **1** (limit of quantification ~1.0:0.2 to ~1.0:4.0 equiv for **1**/NaOH) exhibiting an anomalous increase in last additions of NaOH due to AIEE effect where the stacked species

underwent self-aggregation. Also, because of shift toward red region, it denoted aggregation in a slipped manner (J–aggregation). Inset shows magnified region of the last few additions (~3.4 to 4.0 equiv of NaOH); (d) Fluorescence spectra of **1** with increasing dilution; (e) Fluorescence spectra of **1** (*c*, 5.0 x 10^{-5} M) and **1**+NaOH (excess) and; (f) Fluorescence spectra of **IGM** with increasing dilution.

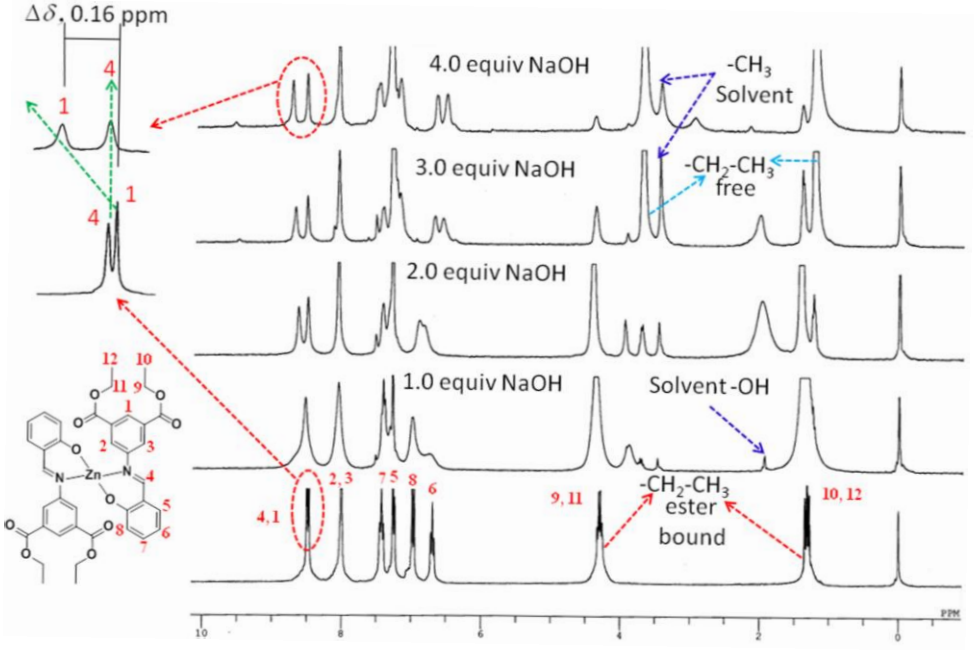

(a)

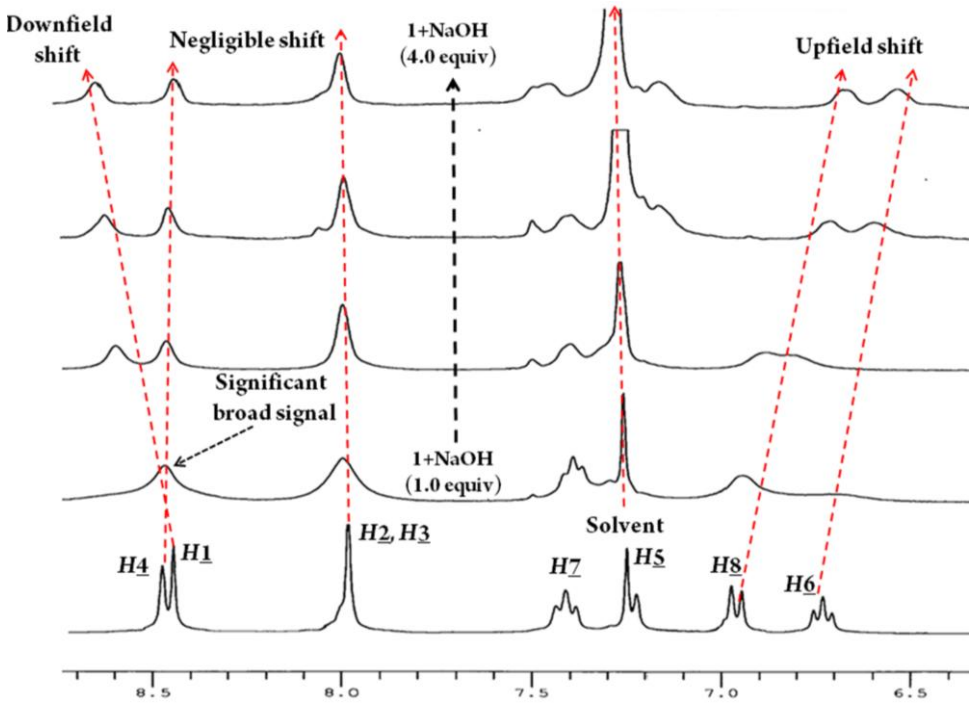

(b)

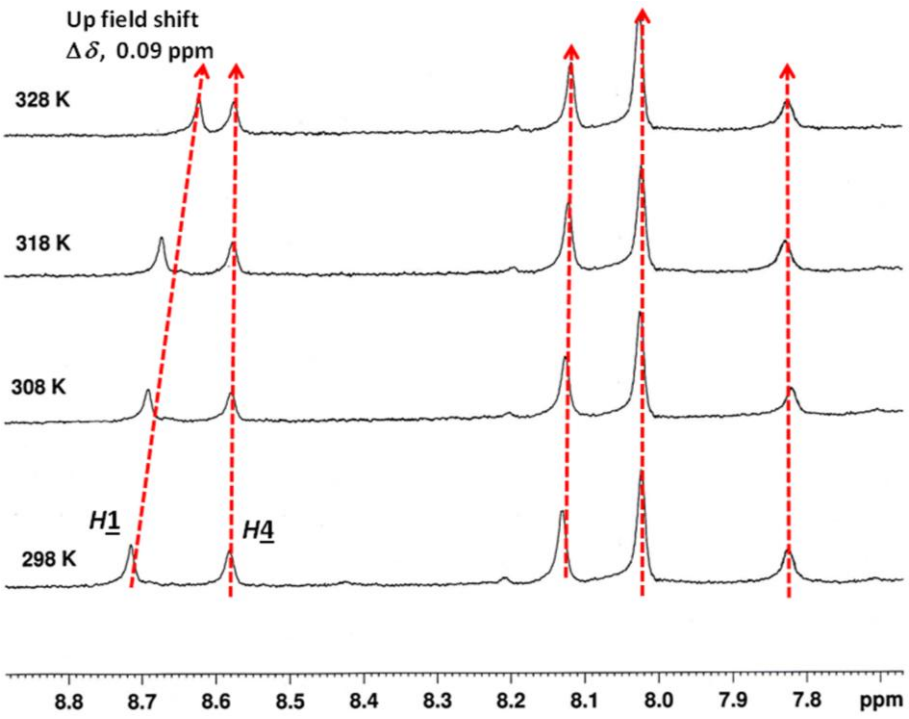

(c)

Figure S8. (a) ^{1}H NMR titration spectrum for **1** *vs* NaOH. The inset on left corner (top) shows criss-crossing of the isophthalate proton (*H*1) over unshifted aldimine proton (*H*4). Besides, residual signals for solvents and fragmented byproducts have been duly interpreted; (b) A portion of ^{1}H NMR titration of **1** *vs* NaOH showing criss-crossing for *H*1 over *H*4, signal broadening at 1.0 equiv of NaOH and a clear display of significant shift (downfield, *H*1; upfield, *H*8 and *H*6) during the titration and; (c) Partial overlay image of temperature dependent ^{1}H NMR experiment of **IGM** which supports the involvement of isophthalate ring in π–stacking.

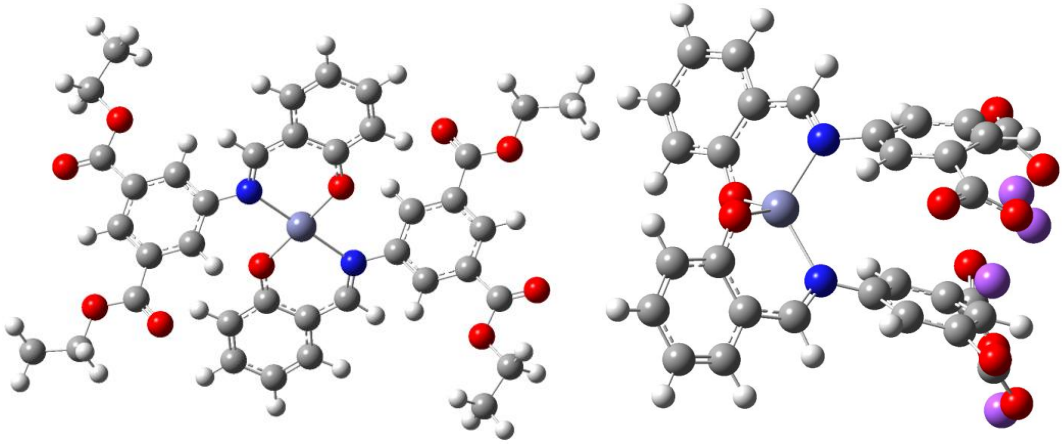

(a) (b)

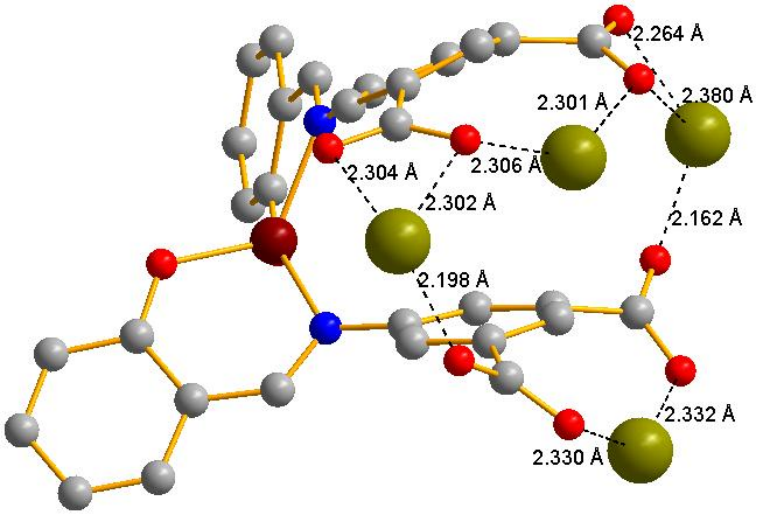

(c)

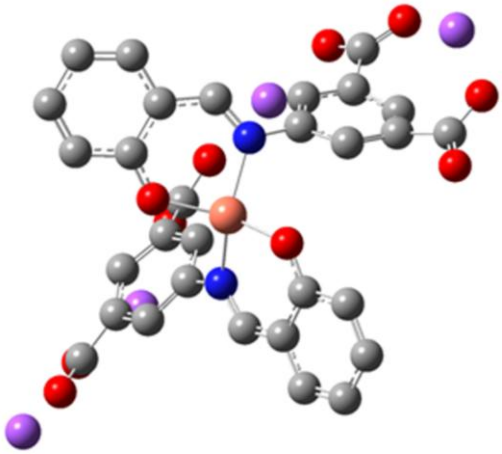

(d)

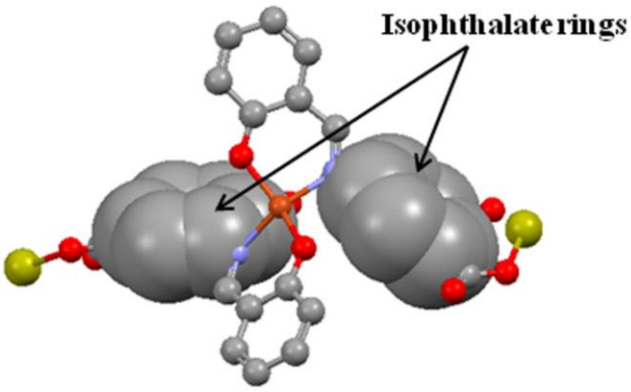

(e)

Figure S9. (a) Optimized structure of **1**; (b) Optimized structure of the corresponding carboxylate Na^{+}-salt (**2**). The HOMO-LUMO energy gap for **1** and **2** converged to be 64.22 eV and 33.20 eV, respectively. Such a large energy gap supported absorption characteristics of **1** and **2** (large bathochromic shift of 41 nm) in the UV/vis spectra; (c) The involvement and stabilization of Na^{+} ions in complex **2**; (d) Optimized structure of Cu^{2+} analogue of **2** and; (e) Optimized structure of Cu^{2+} analogue of **2** showing that isophthalate rings are conformationally not suitable to interact with each other *via* π- interactions which probably prevents the Cu^{2+}, Ni^{2+} and Co^{2+} analogues of **2** to undergo gelation.

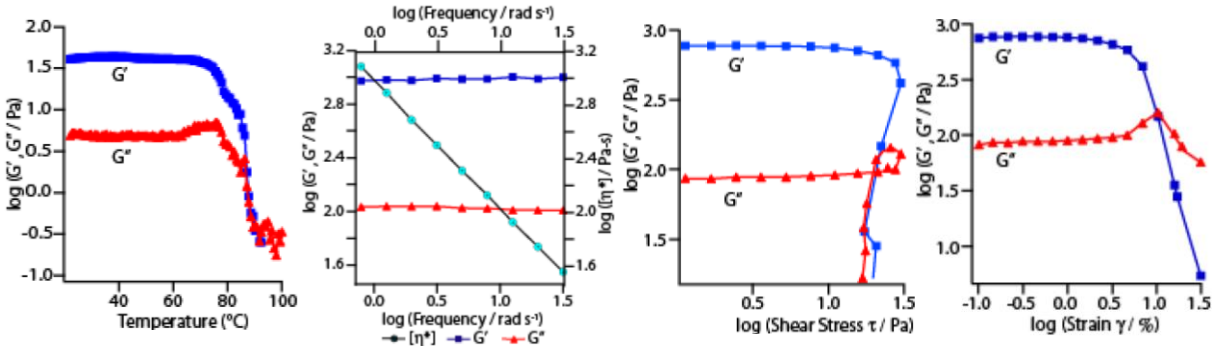

(a) (b) (c) (d)

Figure S10. (a) Storage modulus (G′) and loss modulus (G″) in the temperature range 22 – 100 °C; (b) Primary axis: Dynamic frequency sweep for G′ and G″ for gel, at strain of 0.5%; Secondary axis: complex viscosity; (c) Dynamic shear stress of G′ and G″ for **IGM** at frequency of 1 rad s^{-1} and 22 °C and; (d) Dynamic frequency sweep for G′ and G″ for gel with the applied strain.

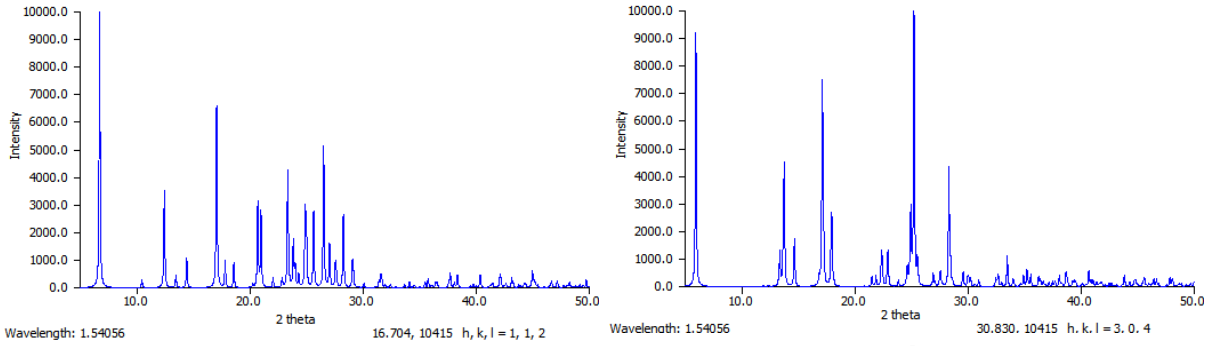

(a) (b)

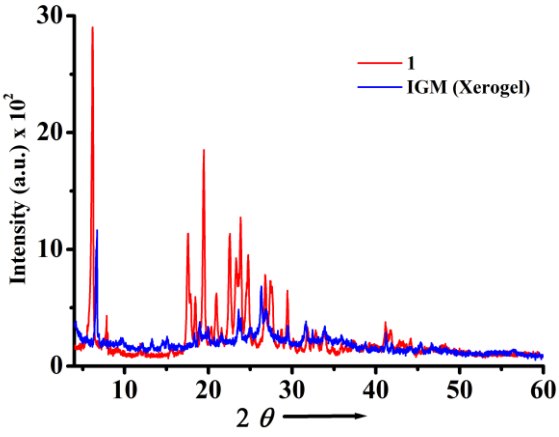

(c)

Figure S11. Powder X-ray diffraction pattern of (a) **HL** and; (b) Copper(II) analogue [$Cu(L_2)$] obtained from their crystal structures; (c) PXRD pattern of complex **1** and vacuum

dried **IGM** (xerogel). The intensity of **IGM** diminished very significantly relative to **1** which clearly suggests that gel material is '*amorphous*'. However, residual NaOH and *in–situ* generated Na^+-salts [Na_2CO_3, $NaOC_2H_5$ etc.] after drying cannot be ruled out in the PXRD pattern of gel (**IGM**).

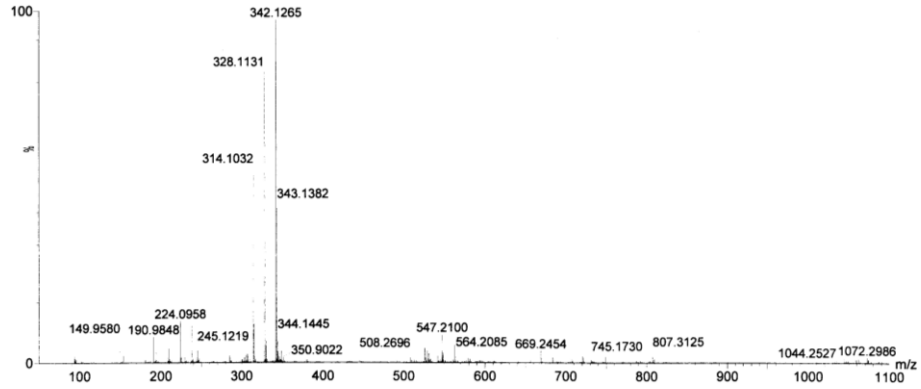

(a)

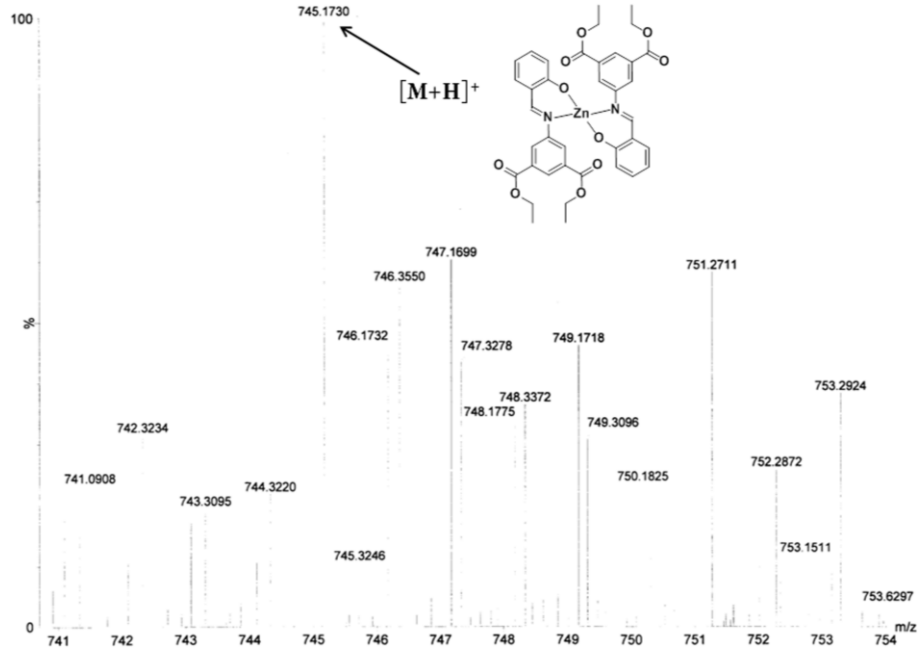

(b)

Figure S12. ESI-Mass spectra of complex (**1**). The molecular ion peak [$(M+H)^+$]; Calcd, found: *m/z*, 745.1740, 745.1730.

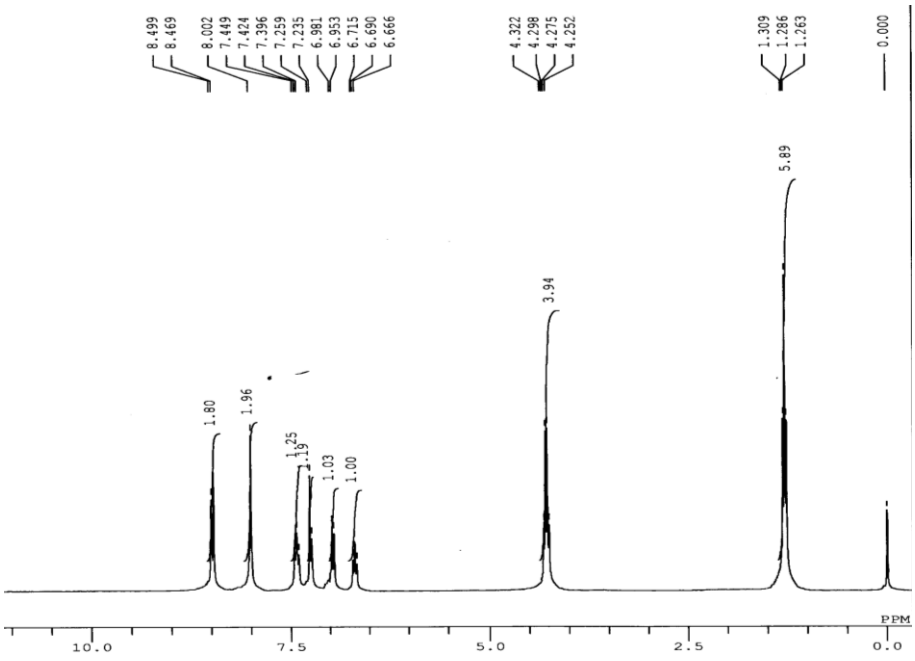

(a)

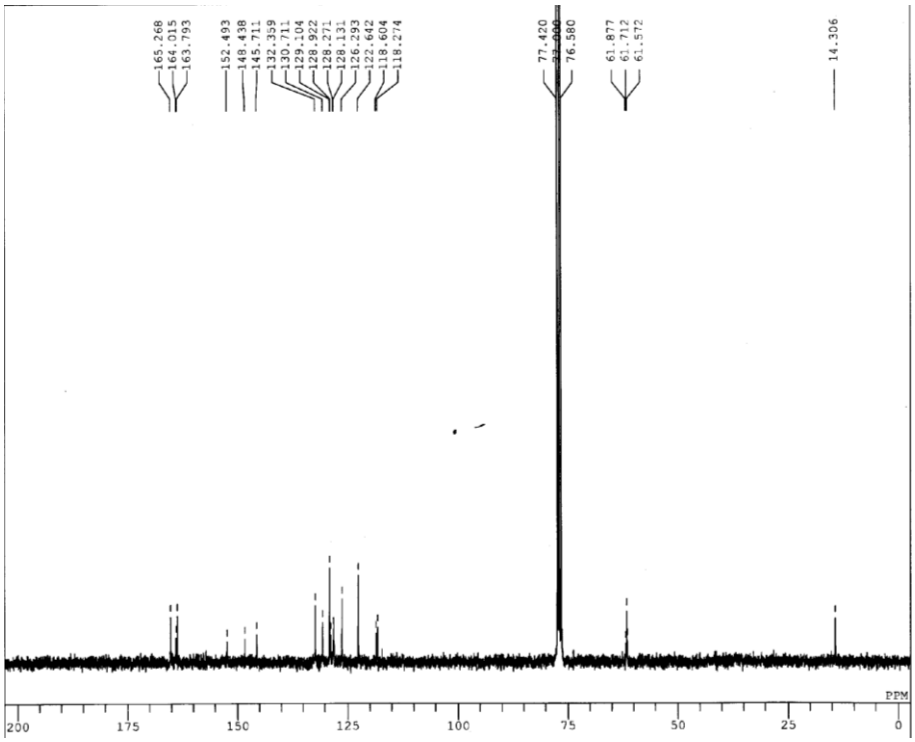

(b)

Figure S13. ^{1}H NMR (a) and ^{13}C NMR spectrum (b) of **1**.

Table S1. The solubility and gelation ability of complex (**1**) [$Zn(L_2)$] in common organic solvents.

Solvents	**Solubility at GC***	**State on addition of NaOH (4.0 equiv) at rt**
Chloroform	Soluble	Gel
Tetrahydrofuran	Soluble	Gel
Dichloromethane	Soluble	Gel
n-Hexane	Insoluble	–
Cyclohexane	Insoluble	–
Benzene	Insoluble	–
Methanol	Insoluble	–
Ethanol	Insoluble	–
Acetonitrile	Insoluble	–
Ethyl acetate	Insoluble	–
Toluene	Insoluble	–
Dimethylformamide	Suspension	Sol
Dimethylsulphoxide	Suspension	Sol
Dioxane	Insoluble	–

*Gelation concentration i.e. 2.0×10^{-2} M.

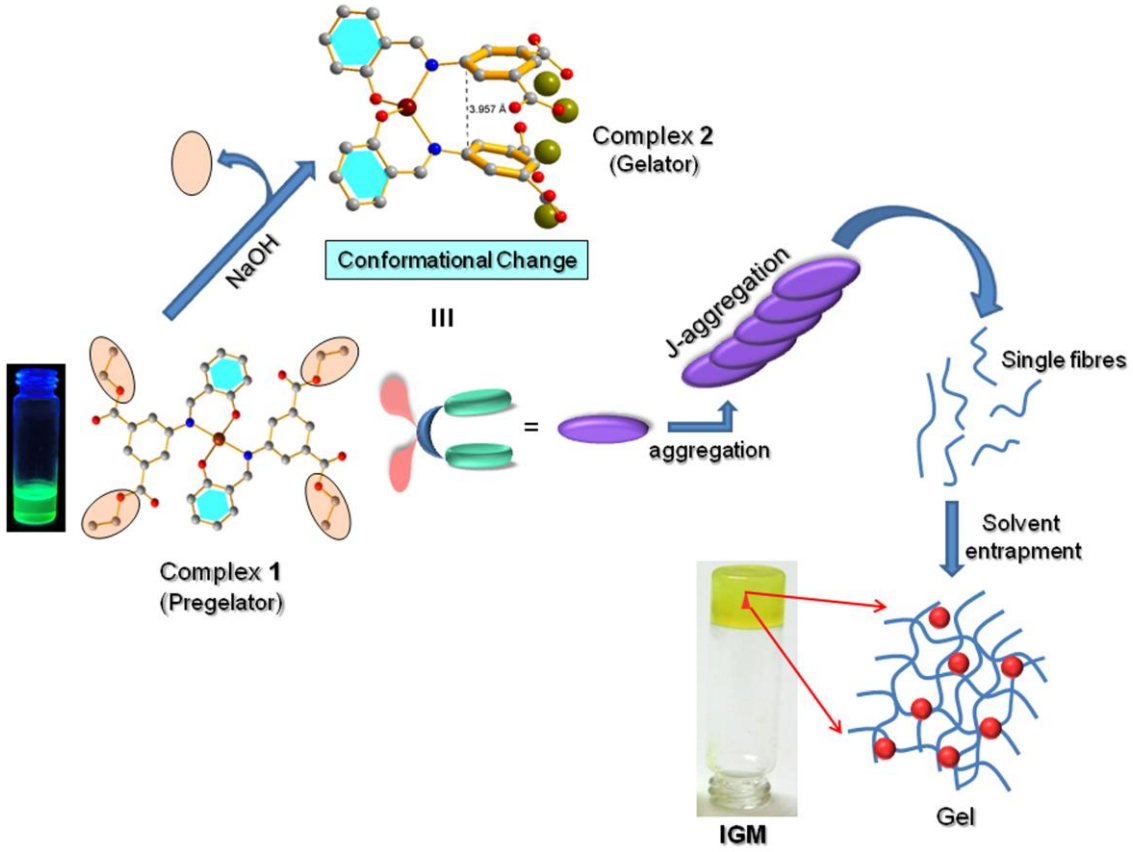

Figure S14. A schematic route for the synthesis of gel and and it's properties as well as correlation with each other in logical steps; The optimized structure of complex **1** undergoes conformational change in presence of NaOH. Removal of the ester fragments induced a significant change in geometry around the central metal Zn(II) from square planar to tetrahedral which offered enhanced π–π/cation–π and other weak interactions. Further, structure in presence of solvated Na^+ involved in π–stacking in a slipped manner that leads to J-aggregates [responsible for significant red shifts in UV/vis (41 nm) and fluorescence (16 nm) spectra]. Further, the J-aggregates assemble into fibres and trap the solvent molecules to form an inorganic gel material (**IGM**).

References

1. D. D. Perrin, W. L. F. Armango, D. R. Perrin, *Purification of Laboratory Chemicals;* Pergamon: *Oxford, U.K.* **1986**.

2. A. Kumar, M. Dubey, R. Pandey, R. K. Gupta, A. Kumar, A. Kalita and D. S. Pandey, *Inorg. Chem*., 2014, **53**, 4944.

3. L. J. Bartolottiand and K. Fluchick, *In Reviews in Computational Chemistry*; K. B. Lipkowitz and D. Boyd, Ed. VCH: New York, 1996, **7**, 187.

4. (*a*) P. Hay and W. R. Wadt, *J. Chem. Phys*., 1985, **82**, 270; (*b*) W. R. Wadt and P. Hay, *J. Chem. Phys.*, 1985, **82**, 284; (*c*) P. Hay and W. R. Wadt, *J. Chem. Phys*., 1985, **82**, 299.

5. M. J. Frisch, G. W. Trucks, H. B. Schlegel, G. E. Scuseria, M. A. Robb, J. R. Cheeseman, G. Scalmani, V. Barone, B. Mennucci, G. A. Petersson, H. Nakatsuji, M. Caricato, X. Li, H. P. Hratchian, A. F. Izmaylov, J. Bloino, G. Zheng, J. L. Sonnenberg, M. Hada, M. Ehara, K. Toyota, R. Fukuda, J. Hasegawa, M. Ishida, T. Nakajima, Y. Honda, O. Kitao, H. Nakai, T. Vreven, J. A. Montgomery, Jr., J. E. Peralta, F. Ogliaro, M. Bearpark, J. J. Heyd, E. Brothers, K. N. Kudin, V. N. Staroverov, R. Kobayashi, J. Normand, K. Raghavachari, A. Rendell, J. C. Burant, S. S. Iyengar, J. Tomasi, M. Cossi, N. Rega, J. M. Millam, M. Klene, J. E. Knox, J. B. Cross, V. Bakken, C. Adamo, J. Jaramillo, R. Gomperts, R. E. Stratmann, O. Yazyev, A. J. Austin, R. Cammi, C. Pomelli, J. W. Ochterski, R. L. Martin, K. Morokuma, V. G. Zakrzewski, G. A. Voth, P. Salvador, J. J. Dannenberg, S. Dapprich, A. D. Daniels, Ö. Farkas, J. B. Foresman, J. V. Ortiz, J. Cioslowski, and D. J. Fox, *Gaussian 09, revision A.1, Gaussian, Inc., Wallingford, CT,* **2009**.

6. A. Das, R. Thakur, A. Dagar and A. Chakraborty, *Phys.Chem.Chem.Phys*., 2014, **16**, 5368.